Intelligent Power Sharing of DC Isolated Microgrid Based on Fuzzy Sliding Mode Droop Control

Mi, Y.; Zhang, H.; Fu, Y.; Wang, C.; Loh, P. C.; Wang, P.

Published in:
IEEE Transactions on Smart Grid

DOI (link to publication from Publisher):
10.1109/TSG.2018.2797127

Publication date:
2019

Document Version
Accepted author manuscript, peer reviewed version

This article has been accepted for publication in a future issue of this journal, but has not been fully edited. Content may change prior to final publication. Citation information: DOI 10.1109/TSG.2018.2797127, IEEE Transactions on Smart Grid

Intelligent Power Sharing of DC Isolated Microgrid Based on Fuzzy Sliding Mode Droop Control

Yang Mi, *Member*, *IEEE,* Han Zhang, *Student Member*, *IEEE*, Yang Fu*, *Member*, *IEEE*, Chengshan Wang, *Senior Member*, *IEEE*, Poh Chiang Loh, *Senior Member*, *IEEE*, Peng Wang, *Senior Member*, *IEEE*

***Abstract*—Linear droop control can realize power sharing among generators in DC microgrid without relying on critical communication links. However, the droop relationship between output power and voltage magnitude of renewable power generate system is nonlinear with uncertainties and disturbances from renewable sources and loads in practical DC microgrid. A novel droop scheme is proposed for an isolated DC microgrid to solve the nonlinear problem. The control strategy is proposed by using the Takagi-Sugeno (T-S) fuzzy model and sliding mode algorithm. The nonlinear droop characteristics can be represented by T-S model through taking advantage of locally measured output variables. The sliding mode droop controller is designed for compensating the uncertainties and disturbances to derive accurate power sharing based on T-S fuzzy model. The proposed scheme is proved to be effective under variable operating conditions through PSIM/Matlab simulation.**

***Index Terms*—Droop control, autonomous power sharing, DC microgrid, T-S fuzzy model, sliding mode control (SMC)**

Nomenclature

V_{dc}	Nominal DC bus voltage (V)	V_e	The DC source voltage (V)
S_i	Nominal output power of DG_i (kW)	C_f	Output capitor (uF)
R_{dg}	The inverter resistance of (Ω)	L	The inverter inductance (mH)
R_l	Line resistance (Ω)	w_c	Filter cut-off frequency (rad/s)

I. Introduction

Along with requirements for environmental friendliness, expandability and flexibility, distributed generation has become more attractive for configuring future electrical grids. In order to manage the renewable energy effectively, microgrid (MG) is a suitable way to be researched widely. In general, MG is a cluster of loads and distributed energy resources operating as a controllable local entity [1-4]. Then DC MG has attracted much research interest because of its lower power conversion losses. DC MG also does not need to balance reactive power [5-8] and may be more attractive for remote or military grids which supply reliability and quality can be more easily ensured.

Such as AC MG, DC MG can also work in isolated mode and grid-connected mode. And there are many DGs, loads and energy storages in MG through power electronic devices. In order to take full use of renewable DGs, many control techniques and power management strategies have been proposed to achieve optimized microgrid operation in terms of reliability, stability, quality, economy and efficiency. Especially, when converter outage occurs, in order to avoid undesirable overloading and assure satisfied voltage regulation, it is important for DGs to share the total load proportionally therefore MG can be centrally controlled as in [2], the power quality can be improved. However, it needs fast communication links, which can increase the cost and reduce the reliability for single points of failure.

Based on the analysis, decentralized droop control has been developed for both AC and DC MGs [9-11]. Therefore linear droop characteristic is built into each DG for linearizing its output power according to terminal voltage [5]. Different sources can supply loads jointly in the DC MG based on their power ratings without relying on any communication links. A distributed droop control has hence been proposed for its "plug and play" characteristic [12-22], but there exist power sharing accuracy problem because it quite depends on line parameters between the DGs and loads. So there exist power sharing errors by using of the conventional droop coefficient [21-22], which can influence DC MG stability operation. Because the local DC voltage of each DG is the only index as in DC MG, which is dependent on line impedance and is used for coordinating active power sharing. These errors can be reduced by adaptive droop coefficients according to system parameters change [16, 20].

The different kinds of droop coefficient optimization methods for DC MG have been studied. One way is to insert additional virtual output impedance for improving both power sharing and stability [4]. Another method is to make each DC DG inject a small AC signal, and then the frequency can be used for active power sharing coordination [12]. The load sharing accuracy can also be enhanced by a low bandwidth communication network for the interchange of the DC voltage and current information between the converter controllers, while the communication delay must be considered [13]. An alternative static droop compensator is thus utilized for power sharing improvement in [14]. This scheme is applied to optimize the droop coefficients by intelligent and robust techniques like Takagi-Sugeno fuzzy method, adaptive method, sliding mode techniques and so on [23, 25]. The adaptive neuro-fuzzy inference system is used for improving the general droop dynamic behavior in [24]. However, the control technique depends on large amount of real training data for covering total load changes [25].

Therefore the novel droop control strategy is designed to optimize the conventional droop coefficient by using local variables such as DC voltage magnitude and DG output power which are usually nonlinear relationship in practice. The proposed droop expressions can be modeled by taking advantage of the T-S fuzzy [26-28] method. Then the droop sliding mode compensation is designed by using the T-S model [29-32], which can provide a robust reference drive signal to the converter for assuring system robustness towards disturbances and uncertainties.

The contribution of the proposed power sharing scheme can be concluded as, 1) More accurate power sharing based on realistic droop expression, 2) More adaptive and intelligent because of T-S fuzzy technique application, 3) More robust for the sliding mode compensator. These advantages assure the designed scheme to be used for DC MG with better power sharing precision and without communication dependency. The rest of research includes four sections. Section II includes the related theory formulation and the improved droop model. Section III introduces the designed power

Yang Mi is with Shanghai University of Electric Power, China (e-mail: miyangmi@163.com), Han Zhang is with State Grid Shanghai shinan Electric Power Supply Company, China (e-mail: hannah0109@sina.com), Yang Fu is with Shanghai University of Electric Power, China (e-mail: mfudong@126.com), Chengshan Wang is with Tianjin University, China (e-mail: cswang@tju.edu.cn), P.C. Loh is with Aalborg University, Denmark(e-mail: pcl@et.aau.dk), Peng Wang is with Nanyang Technological University, Singapore (e-mail: epwang@ntu.edu.sg).

*Corresponding author.

This article has been accepted for publication in a future issue of this journal, but has not been fully edited. Content may change prior to final publication. Citation information: DOI 10.1109/TSG.2018.2797127, IEEE Transactions on Smart Grid

sharing controller based on fuzzy sliding mode control. The simulation results are provided in Section IV and the conclusions are drawn in Section V.

II. Modeling of Fuzzy Sliding Mode Droop Control

DC MG only has two independent variables identified respectively as active power and DC terminal voltage, which can be described by linear P-V droop relation and assure the DGs share power proportionally according to their respective power ratings with "plug and play" advantage. Moreover, unnecessary load shedding and source overloading are avoided. However the power sharing accuracy need to be improved for conventional droop scheme, the principles are described as follows.

A. Conventional Droop Scheme

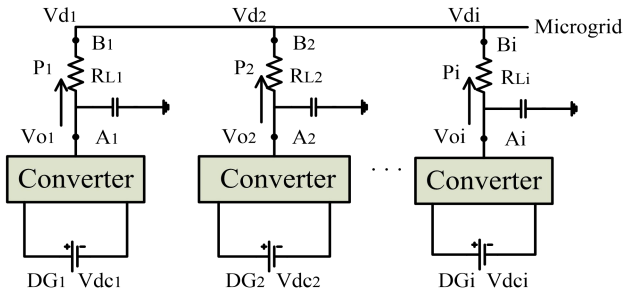

Fig. 1.The power flow of the DC microgrid

In order to explain droop principles, the DC MG with multiple DGs shown in Fig. 1 is considered as an example. For each DG, its DC voltages at points A_i and B_i, separated by line resistance R_{Li}, can be denoted as V_{oi} and V_{di}, respectively, where subscript i represents the source unit number in the DC MG. The inductance can be ignored in the steady-state power sharing and only resistance is considered in DC MG [33]. Instantaneous power P_i from the DG can then be computed as,

$$P_i = V_{oi}(V_{oi} - V_{di}) / R_{Li} \tag{1}$$

It represents the relationship between the output power P_i and the output voltage V_{oi} is nonlinear, the line resistance R_{Li} and the changing value V_{di} are uncertainty because of the load fluctuation. Considering the simplification of the controller design process, the traditional power sharing can be controlled by the linear droop equation as,

$$V_{oi} = V_{mi} - P_i \cdot m_i \tag{2}$$

where V_{mi} represents the maximum source output voltage without load, m_i represents the droop coefficient.

However, in order to derive better power sharing precision when considering the line resistance, the droop method can be modified through adding virtual resistance compensation in the controller design. Therefore equation (2) can be changed as,

$$V_{oi} = V_{mi} - P_i \cdot m_i - i_{oi} \cdot R_d \tag{3}$$

where i_{oi} is the output current and R_d is the inserted virtual resistance.

Although the conventional droop control scheme from equation (2) can work well, its power sharing may be affected by line parameter variations because of the fixed tangent slope along the curve. A large ratio between output power and voltage may have the advantage of better load sharing but sacrifices the regulation stiffness, while a smaller ratio requires smaller droop voltage range but it is more sensitive to be impact from cables and sensors [34].

B. Proposed Droop Model

The improved droop model with a variable slope is proposed to describe practical droop relationship between voltage and output power in this paper. The source rating and DC bus voltage range is predetermined by the system specifications, that is, the start point and the end point of the droop curve is predefined. The only freedom is to design the trajectory between the two points which should satisfy the following two desirable characteristics [34],

1) The curve has larger droop resistance at heavy load, which can assure better load sharing. Otherwise, uneven load sharing leads to source saturation and accelerates the bus voltage drop when the load is heavy.

2) The curve has smaller droop resistance at light load, which can enable tighter voltage regulation. As long as sources are working well within limit, deviation from ideal value is acceptable. The tight voltage regulation with smaller droop resistance is beneficial because higher bus voltage usually leads to smaller current and higher system efficiency.

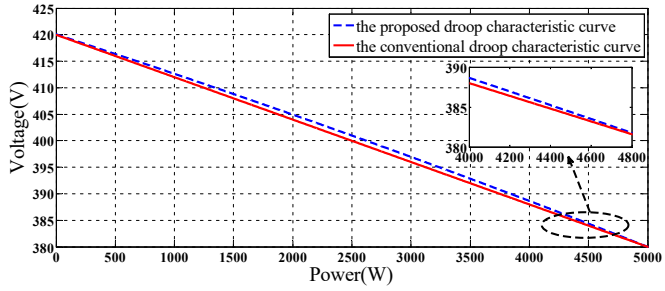

Fig. 2.Droop characteristic curves with two droop methods for same converter

In order to give an intuitive interpretation for droop characteristics, the conventional droop trajectory in equation (2) and the practical droop curves are compared as in Fig 2. The straight line is the conventional droop with model approximation. And the dash parabola curve trajectory which shows the nonlinear droop relationship between ΔP and ΔV could be given by curve fitting as in [34],

$$\begin{aligned}\Delta P &= K_d(\Delta V + V_{op})\Delta V = K_d[\Delta V^2 + (2\times 0.5)V_{op}\Delta V \\ &\quad + (0.5V_{op})^2 - (0.5V_{op})^2] \\ &= K_d[(\Delta V + 0.5V_{op})^2 - 0.25V_{op}^2]\end{aligned} \tag{4}$$

where V_{op} is the voltage magnitude of point A. K_d is the proposed droop coefficient and it is negative

The new model for DC voltage magnitude and active power can hence be deduced as,

$$\Delta V = \pm\sqrt{\Delta P / K_d + 0.25V_{op}^2} - 0.5V_{op} \tag{5}$$

According to the droop characteristic showed in Fig. 2, It is clear that the voltage should decrease when the power increases, and vice versa. It means when ΔP is negative, ΔV must be positive. Therefore, there is only one reasonable solution for equation (4) as

$$\Delta V = \sqrt{\Delta P / K_d + 0.25V_{op}^2} - 0.5V_{op} \tag{6}$$

C. Modeling of Proposed Droop Scheme

The improved droop scheme is used for controlling DG converters interfaced to DC MG. Although these converters may have different topologies, they can be modeled by the same procedure and all converters assumed to have the boost configuration.

Small-signal analysis can be used by taking advantage of droop scheme model and components of converters such as voltage and current controllers. An overview representation of this system is provided in Fig. 3 [35-36]. It can be seen that the power signal is filtered by a low-pass filter for extracting the average power only. This average power is fed to the proposed droop scheme in the power controller for realizing the demanded power sharing. Reference voltage from the power controller is then sent to the voltage controller, which can simply be a Proportional-

This article has been accepted for publication in a future issue of this journal, but has not been fully edited. Content may change prior to final publication. Citation information: DOI 10.1109/TSG.2018.2797127, IEEE Transactions on Smart Grid

Integral (PI) controller. The signal produced by the PI controller is sent to the current controller as reference signal. The current controller output is finally the desired signal for modulating the converter.

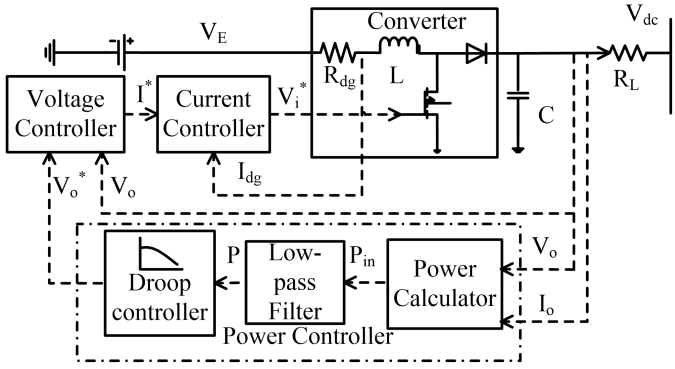

Fig. 3. Block diagram model of VSI

This flow of signals can be modeled mathematically which is the instantaneous power P_{in} expressed in terms of the sampled output voltage and current of the converter,

$$P_{in} = V_o \cdot I_o \tag{7}$$

The first derivative of P which is the low-pass filtered output in the time domain can be formulated as,

$$\dot{P} = \omega_c V_o I_o - \omega_c P \tag{8}$$

where ω_c is the cutoff frequency of the filter. Accordingly, P is a function of V_o and I_o,

$$P = f(V_o, I_o) \tag{9}$$

In order to analyze the small-signal stability of the system in Fig. 3, linearization model around the operating point [35] is performed as (10) and (11).

$$\Delta P = \left.\frac{\partial f}{\partial V_o}\right|(V_{op}, I_{op})\Delta V_o + \left.\frac{\partial f}{\partial I_o}\right|(V_{op}, I_{op})\Delta I_o \tag{10}$$

$$\Delta \dot{P} = -\omega_c \Delta P + \omega_c I_{op}\Delta V_o + \omega_c V_{op}\Delta I_o \tag{11}$$

where ΔP and ΔV_o are chosen as the state variables, I_{op} and V_{op} are the converter output voltage and current at the considered operating point.

According to the proposed droop expression in (6), reference DC voltage from the power controller can then be represented as,

$$V_o^* = V_{op} + \Delta V = \sqrt{(P - P_r)/K_d + 0.25V_{op}^2} + 0.5V_{op} \tag{12}$$

In order to describe the voltage and current control loops, ϕ and φ are defined as state variables by the following equations,

$$d\phi/dt = V_o^* - V_o \tag{13}$$

$$d\varphi/dt = I^* - I_{dg} \tag{14}$$

The outputs of the two PI controllers can thus be represented as,

$$\Delta I^* = k_{Iv}\Delta\phi + k_{Pv}(\Delta V_o^* - \Delta V_o) \tag{15}$$

$$\Delta V_i^* = k_{Ii}\Delta\varphi + k_{Pi}(\Delta I^* - \Delta I_{dg}) \tag{16}$$

According to (12), (15-16), (13) and (14) can be expanded to give the following,

$$\Delta\dot{\phi} = \Delta V^* - \Delta V_o = \sqrt{\Delta P/K_d + 0.25V_{op}^2} - 0.5V_{op} - \Delta V_o \tag{17}$$

$$\begin{aligned}\Delta\dot{\varphi} &= \Delta I^* - \Delta I_{dg} = k_{Iv}\Delta\phi_i - \Delta I_{dg} - k_{Pv}\Delta V_o \\ &+ k_{Pv}(\sqrt{\Delta P/K_d + 0.25V_{op}^2} - 0.5V_{op})\end{aligned} \tag{18}$$

Then, the circuit behaviors of the converter and filter are represented as

$$dI_{dg}/dt = [V_E - R_{dg}I_{dg} - (1 - V_i^*)V_o]/L \tag{19}$$

$$dV_o/dt = [(1 - V_i^*)I_{dg} - I_o]/C \tag{20}$$

The total system state-space model can eventually be established by using (11), (17-20) as follows,

$$\dot{x} = A(x) + Bu \tag{21}$$

where

$$A(x) = \begin{bmatrix} -\omega_c\Delta P + I_{op}\omega_c\Delta V_o; \\ \sqrt{\Delta P/K_d + 0.25V_{op}^2} - 0.5V_{op} - \Delta V_o; \\ k_{Pv}(\sqrt{\Delta P/K_d + 0.25V_{op}^2} - 0.5V_{op}) + k_{Iv}\Delta\phi - k_{Pv}\Delta V_o - \Delta I_{dg} - I_{dgr}; \\ -k_{Pi}k_{Pv}(I_{dgr} + \Delta I_{dg})(\sqrt{\Delta P/K_d + 0.25V_{op}^2} - 0.5V_{op})/C + \Delta I_{dg}/C \\ -k_{Pi}k_{Iv}\Delta\phi(I_{dgr} + \Delta I_{dg})/C - k_{Ii}\Delta\varphi(I_{dgr} + \Delta I_{dg})/C + I_{dgr}/C \\ +k_{Pi}k_{Pv}\Delta V_o(I_{dgr} + \Delta I_{dg})/C + [k_{Pi}(I_{dgr} + \Delta I_{dg})^2 - I_{op} - \Delta I_o]/C; \\ k_{Pi}k_{Pv}(V_{op} + \Delta V_o)(\sqrt{\Delta P/K_d + 0.25V_{op}^2} - 0.5V_{op})/L - V_{op}/L \\ +k_{Pi}k_{Iv}\Delta\phi(V_{op} + \Delta V_o)/L + k_{Ii}\Delta\varphi(V_{op} + \Delta V_o)/L - R_{dg}\Delta I_{dg}/L \\ -k_{Pi}k_{Pv}\Delta V_o(V_{op} + \Delta V_o)/L - k_{Pi}\Delta I_{dg}(V_{op} + \Delta V_o)/L \\ -k_{Pi}I_{dgr}(V_{op} + \Delta V_o)/L + V_E/L - R_l I_{dgr}/L - \Delta V_o/L; \end{bmatrix}$$

$B = [\omega_c V_{op} \quad 0 \quad 0 \quad -1/C \quad 0]^T$,

$x = [\Delta P \quad \Delta\phi \quad \Delta\varphi \quad \Delta V_o \quad \Delta I_{dg}]^T$, $u = [\Delta I_o]$.

The state vector of DC MG in (21) includes the state variables of the converter, passive components and control system, respectively notated as ΔP, $\Delta\phi$, $\Delta\varphi$, ΔV_o and ΔI_{dg}. Although it is simplified, the state model is nonlinear in fact and is hence difficult to be controlled by a traditional PI controller.

III. Power Sharing Based on Proposed Droop Scheme

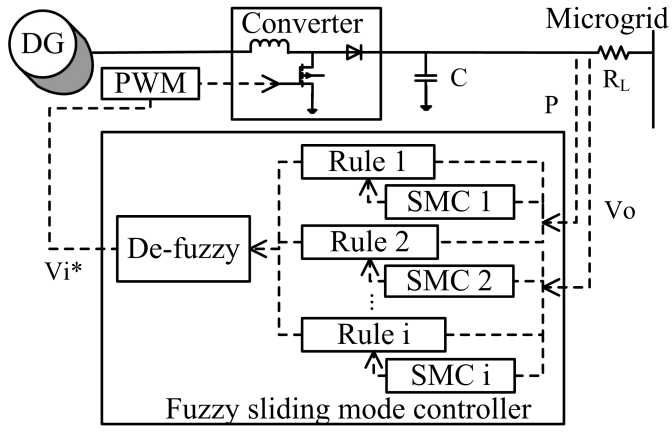

Fig.4. The DG control block diagram based on the fuzzy sliding mode control

In order to obtain better power sharing accuracy which is affected by parameter uncertainties and load disturbance with no communication between the droop controllers, a fuzzy sliding mode droop scheme is designed for DC MG. The T-S fuzzy model can be used for representing the nonlinear droop relation based on the local measurement quantities such as DG output power and DC voltage magnitude. The sliding mode droop control can then

This article has been accepted for publication in a future issue of this journal, but has not been fully edited. Content may change prior to final publication. Citation information: DOI 10.1109/TSG.2018.2797127, IEEE Transactions on Smart Grid

be designed for improving robustness because of parameter uncertainties and operating condition variation. The output signal from the fuzzy sliding mode droop controller is eventually sent to the pulse-width modulator. More details related to the controller design are provided as Fig. 4.

A. T-S Fuzzy Model

The proposed droop model in (21) can be described as T-S fuzzy rules by several simple linear systems developed by feeding the converter output power according to Fig. 4. [28-32, 37].

Plant Rule i (i=1,2...r) [26]-[28]

If $\Delta P_i(t)$ is μ_1^i, $\Delta V_o(t)$ is μ_2^i, then

$$\dot{x}(t) = (A_i + \Delta A_i)x(t) + B_i u(t) + d(t) \tag{22}$$

where Rule $i = 1,2,\cdots,q$ denotes the i_{th} fuzzy inference rule, $\Delta P_i(t)$ and $\Delta V_o(t)$ are the premise variables, μ_1^i and μ_2^i are fuzzy sets, n is the number of premise variables, $x(t) \in R^n$ is the state vector, $u(t) \in R^m$ is the control input vector, $d(t)$ is the system disturbance vector, $A_i \in R^{n\times n}$ and $B_i \in R^{n\times m}$ are the system matrix and input matrix, respectively, and ΔA_i is the time-varying matrix with appropriate dimensions for representing parametric uncertainties in the plant model.

The global fuzzy model is obtained by fuzzy aggregation of each individual rule as follows [27-28]:

$$\dot{x}(t) = \frac{\sum_{i=1}^{q} \mu_i(x(t))\{(A_i + \Delta A_i)x(t) + B_i u(t) + d(t)\}}{\sum_{i=1}^{q} \mu_i(x(t))} \tag{23}$$

Some basic properties of $\mu_i(x(t))$ are $\mu_i(x(t)) \geq 0$, and $\sum_{i=1}^{q} \mu_i(x(t)) \geq 0$. Define $h_i(x(t)) = \mu_i(x(t)) \Big/ \sum_{i=1}^{q} \mu_j(x(t))$, the defuzzified output of the T-S fuzzy system (23) can be represented as follows.

$$\dot{x}(t) = \sum_{i=1}^{q} h_i(x(t))[A_i x(t) + \Delta A_i x(t) + B_i u(t) + d(t)] \tag{23'}$$

In order to prove conveniently, the total uncertainty is defined as $f_i(x,t) = \Delta A_i x(t) + d(t)$ which is the set of the nonlinear part of the system model and the system uncertainties. Equation (23') can then be rewritten as:

$$\dot{x}(t) = \sum_{i=1}^{q} h_i(x(t))[A_i x(t) + B_i u(t) + f_i(x,t)] \tag{24}$$

where the membership function $h_i(x(t)) \geq 0$, $\sum_{i=1}^{q} h_i(x(t)) = 1$.

B. Sliding Mode Droop Controller Design

In order to design global sliding mode droop controller conveniently for the T-S fuzzy model developed from the original droop control system, the following assumptions and definitions are introduced.

A1: All the matrices $B_i, i = 1,\cdots,r$ are the same, i.e, $B_1 = B_2 = \cdots = B_r = B$. Furthermore, suppose that the matrix B is of full-column rank, A_i and B_i are both fully controllable.

A2: Disturbance $f_i(x,t)$ is viewed as bounded. That means there exists a known scalar D such that $\|f_i(x,t)\| \leq D$, where $\|\cdot\|$ is a matrix norm.

Definition 1: If the pairs (A_i, B), $i = 1,2,\cdots,r$ are controllable, the fuzzy system (24) is said to be locally controllable [29-30].

Definition 2: For a scalar variable s, the following expression is defined,

$$\operatorname{sgn} s = \begin{cases} 1, & \text{when s>0} \\ 0, & \text{when s=0} \\ -1, & \text{when s<0} \end{cases}$$

For a vector variable $s \in R^m$, the following alternative expression is defined.

$$\operatorname{sgn} s = [\operatorname{sgn} s_1, \operatorname{sgn} s_2, \cdots, \operatorname{sgn} s_m]^T$$

Based on the T-S fuzzy approximated system in (24), the sliding mode controller is designed in two general procedural steps as the desired sliding surface selection and the design of sliding mode control.

(1). Design of Sliding Surface

The switching function and surface are defined as:

$$s_i(t) = C_i x(t) - \int_0^t \sum_{i=1}^{q} h_i(\mathrm{x}(\tau))(C_i A_i - C_i B_i K_i)x(\tau) d\tau \tag{25}$$

$$S_i = \{\tilde{x} \in R^n : C_i x(t) = 0\} \tag{26}$$

where C_i and K_i are constant matrices, matrix C_i is then chosen to assure that $C_i B_i$ is nonsingular, while matrix K_i is designed by pole assignment to make the eigenvalues of $A_i - B_i K_i$ less than zero.

The dynamic trajectory of the system, when restricted on the sliding surface, will satisfy the following equation.

$$s_i(t) = 0 \text{ and } \dot{s}_i(t) = 0 \tag{27}$$

According to $\dot{s}_i(t) = 0$, the equivalent controller can be represented as,

$$u_{ieq}(t) = -(C_i B_i)^{-1} \sum_{i=1}^{q} h_i(x(t))[C_i B_i K_i x(t) + C_i f_i(x,t)] \tag{28}$$

Substituting (28) to (24), the equivalent dynamic equation in the sliding mode can further be expressed as:

$$\begin{aligned} \dot{x}(t) = \sum_{i=1}^{q} h_i(x(t)) \sum_{j=1}^{q} h_j(x(t))[(A_i - B_i K_i)x(t) \\ + (I - B_i(C_i B_i)^{-1} C_i) f_i(x,t)] \end{aligned} \tag{29}$$

where K_i is chosen such that $(A_i - B_i K_i)$ has stable eigenvalues. By using the equivalent controller $u_{ieq}(t)$, the state trajectory can be controlled as the desired sliding mode $s_i(t) = 0$. Suppose there are positive-definite matrixes P and W, which satisfy the Lyapunov equation as follows:

$$P(A_i - B_i K_i) + (A_i - B_i K_i)^T P = -W \tag{30}$$

Theorem 1: If A2 is satisfied, and $\|x\| \geq \frac{2D_1\|P\|}{\|W\|}$ for all t, the system dynamic performance in sliding mode is always stable.

Proof: The Lyapunov function approach is one of the methods for specifying the stability of the sliding surface. Select the Lyapunov function as,

This article has been accepted for publication in a future issue of this journal, but has not been fully edited. Content may change prior to final publication. Citation information: DOI 10.1109/TSG.2018.2797127, IEEE Transactions on Smart Grid

$$v = x(t)^T Px(t). \tag{31}$$

Then, the derivative of v shown in (31) along the trajectory (29) is given as follows.

$$\begin{aligned}\dot{v} &= \sum_{i=1}^{r} h_i(x(t))x(t)^T P[A_i x(t) + B_i u_{ieq}(t) + f_i(x,t)] \\ &+\sum_{i=1}^{r} h_i(x(t))[A_i x(t) + B_i u_{ieq}(t) + f_i(x,t)]^T Px(t) \\ &= \sum_{i=1}^{r} h_i(x(t))\{x(t)^T[(A_i - B_i K_i)^T P + P(A_i - B_i K_i)]x(t) \\ &+[(I - B_i(C_i B_i)^{-1} C_i) f_i(x,t)]^T Px \\ &+x^T P[(I - B_i(C_i B_i)^{-1} C_i) f_i(x,t)]\}\end{aligned} \tag{32}$$

From A2, $\left\|(I - B_i(C_i B_i)^{-1} C_i) f_i(x,t)\right\| \le D_1$ can be defined, then

$$(32) \le \sum_{i=1}^{r} h_i(x(t))\{-\|W\|\|x(t)\|^2 + 2D_1\|P\|\|x(t)\|\} \tag{33}$$

By using the inequality in Theorem 1, $\dot{v} < 0$ can be concluded.

(2). Design of Sliding Mode Controller

The sliding control law composes the equivalent control law and switching control law as following.

$$u_i(t) = u_{ieq}(t) + u_{i0}(t) \tag{34}$$

The equivalent controller is derived from (28) when the state trajectory reaches the sliding surface. In contrast, the switching control is designed using the following reaching law,

$$u_{io}(t) = \dot{s}_i(t) = -\beta_1 s_i(t) - \beta_2 \operatorname{sgn}(s_i(t)) \tag{35}$$

where β_1 and β_2 are two positive numbers. β_1 is related to the response time and β_2 is about the stable precision of the system.

The following sliding mode controller can then be defined by using (24), (28) and (35).

$$\begin{aligned}u_i(t) = &-(C_i B_i)^{-1}\sum_{i=1}^{q} h_i(x(t))[C_i B_i K_i x(t) + C_i D] \\ &-\beta_1 s_i - \beta_2 \operatorname{sgn} s_i\end{aligned} \tag{36}$$

Theorem 2: If the decentralized switching control law in (36) is designed, the hitting condition is satisfied.

Proof: Here it is needed to prove the trajectory of the system reaching the switching surface S in finite time, and stay on it which is assured by (36).

The derivative of s along the system of (24) and (36) as,

$$\begin{aligned}\dot{s}_i &= C\dot{x}_i(t) = C_i\sum_{i=1}^{q} h_i(x_i(t))[A_i x_i(t) + B_i u_i(t) + f_i(x,t)] \\ &= C_i\sum_{i=1}^{q} h_i(x(t))[A_i x_i(t) + f_i(x,t)] \\ &-C_i B_i\{(C_i B_i)^{-1}\sum_{i=1}^{q} h_i(x_i(t))[C_i B_i K_i x(t) + C_i D] \\ &+\beta_1 s_i + \beta_2 \operatorname{sgn} s_i\} \\ &\le -C_i B_i(\beta_1 s + \beta_2 \operatorname{sgn} s)\end{aligned} \tag{37}$$

In order to prove the hitting condition is satisfied, $s_i^T \dot{s}_i < 0$ should be tested,

$$\begin{aligned}s_i^T \dot{s}_i(t) &= -\beta_1 s_i^T C_i B_i s_i - \beta_2 s_i^T C_i B_i \operatorname{sgn} s_i \\ &\le -\beta_1\|C_i\|\|B_i\|\|s_i\| - \beta_2\|C_i\|\|B_i\|\sum_{j=1}^{m}|s_{ij}|\end{aligned} \tag{38}$$

Inequality (38) shows $s^T \dot{s} < 0$ which assure the system trajectories reach the hitting condition in finite time and stay on it. So the stability of the proposed sliding mode control system is proved with Lyapunov stability theory.

C. Summarized Procedure

The proposed sliding mode compensation droop controller is designed through three steps summarized as follows,

1) Construct state equation for representing the practical droop relationship. Then the range of ΔP and operation points are deduced from the equation trajectories.

2) Apply T-S fuzzy technique to approximate the nonlinear droop equation by using the system operation points and the Gauss membership function for droop compensator design.

3) Design of sliding mode droop controller by selecting the switch function and reaching condition based on poles placement and Lyapunov method.

IV. Case Study

The DC MG with three DG converters as in Fig. 5 is simulated by using PSIM/Matlab software. In order to test the effective of the designed control scheme, the traditional droop method, the droop scheme with virtual resistance and the proposed droop are compared in the following cases.

The DG nominal ratings are set as 5kW for DG1, 10kW for DG2 and 15kW for DG3. Each DG is simulated as a DC power supply, connected to the 400V DC bus through a converter. Other parameters used for the simulation are provided in Appendix A. Three output voltage references from the droop model are added to the power controller.

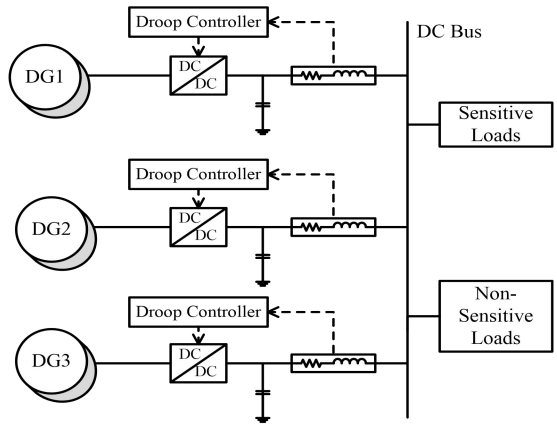

Fig. 5.Microgrid structure

Taking DG1 as an example, its trajectory is shown in Fig. 6 with initial condition x(0)=[-1 -1 -1 -1 -1]^T. The range of variable ΔP and ΔV_o is between $[-5000, 5000]\times[-400, 400]$. In order to cover this region in the phase plane, fuzzy rules can be selected according to the operating points at (-5000, 20, -25), (-1666, 6.664, -8.064), (1666, -6.664, 8.894) and so on [26].

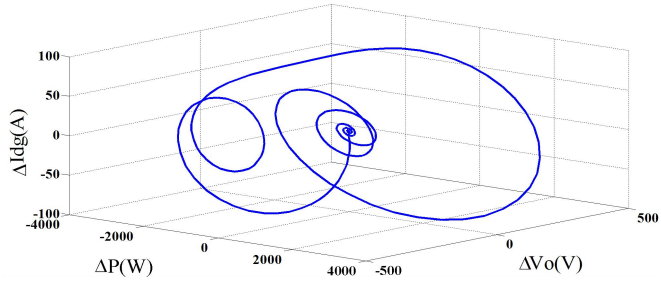

Fig. 6.Trajectory of the DG1 control system in the phase plane

Plant Rule i (i=1,2...16)

If $\Delta P_1(t)$ is μ_1^i, $\Delta V_o(t)$ is μ_2^i, then

$$\dot{x}(t) = (A_i + \Delta A_i)x(t) + B_i u(t) + d(t)$$

This article has been accepted for publication in a future issue of this journal, but has not been fully edited. Content may change prior to final publication. Citation information: DOI 10.1109/TSG.2018.2797127, IEEE Transactions on Smart Grid

where μ_1^i and μ_2^i can be seen in the below table.

ΔP \ ΔV_o	20	6.664	-6.664	-20
-5000	Rule 1	Rule 2	Rule 3	Rule 4
-1666	Rule 5	Rule 6	Rule 7	Rule 8
1666	Rule 9	Rule 10	Rule 11	Rule 12
5000	Rule 13	Rule 14	Rule 15	Rule 16

The membership functions of ΔP and ΔV_o can be chosen as the Gauss function [37-38] shown in Fig. 7. The detailed fuzzy model of DG1 can be found in Appendix B.

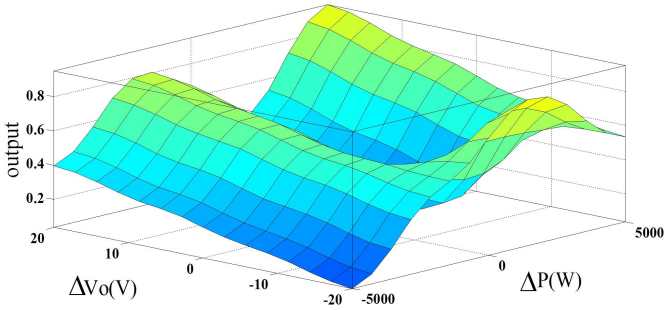

Fig. 7.The fuzzy logic surface

The poles of DG1 can be placed under each fuzzy rule to obtain the matrix C_i of switching surface function for DG1 [26]. Take C_1 to C_3 as examples,

$$C_1 = [247.6584 \quad 13.2125 \quad -2.6508 \quad -0.0036 \quad 1.0000],$$
$$C_2 = [222.6874 \quad 18.3299 \quad -2.5469 \quad -0.0034 \quad 1.0000],$$
$$C_3 = [202.3258 \quad 25.4068 \quad -2.4762 \quad -0.0032 \quad 1.0000],$$

And the corresponding eigenvalues of $A_i - B_i K_i$ can be found in Appendix. The sliding mode controller can eventually be designed as:

$$u_i(t) = -(C_i B_i)^{-1} \sum_{i=1}^{q} h_i(x(t))[C_i B_i K_i x(t) + C_i D] - \beta_1 s_i - \beta_2 \operatorname{sgn} s_i$$

where the values of β_1 and β_2 are chosen as 13 and 1.3 respectively based on the trials and the experiences [37]. The designed controller can be tested for two cases with different load changes, DG outages and line resistances as follows.

Case 1: Load Changes and DG Outages

In this case, we consider the load changes from 10kW to 8kW at 0.5s and DG1 removed at 1.0s. The working DGs should always share the load in proportion to their ratings, which is 1:2:3. The line resistances of the DGs are set to 0.3Ω, 0.4Ω and 0.5Ω respectively. The voltage magnitudes and output powers of the three DGs under conventional droop control are shown in Fig. 8 - Fig. 9. And the results with the virtual resistance compensation can be seen in Fig. 10 - Fig. 11. The results with the nonlinear droop description and the traditional PI control method are represented in Fig.12- Fig. 13. Considering the limitation of the conventional control method, the power sharing with the nonlinear droop relationship has only made a little improvement than the traditional power sharing and a similar result with the load sharing with the virtual resistance. However the nonlinear droop curve could describe the realistic relationship better that a little difference between the two descriptions of the droop relationship might result in a significant gap of the power sharing.

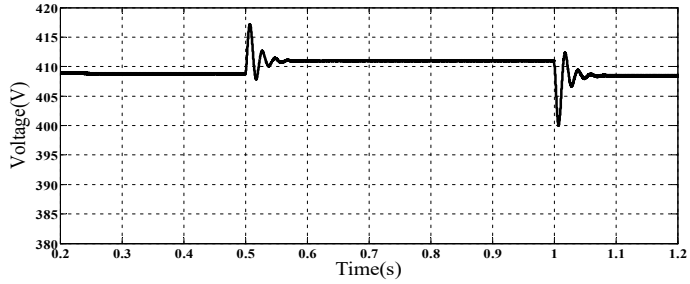

Fig. 8.The voltage variation with the conventional droop control in Case 1

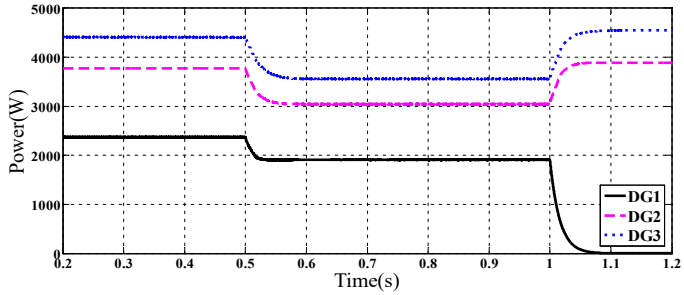

Fig. 9.The power sharing with the conventional droop control in Case 1

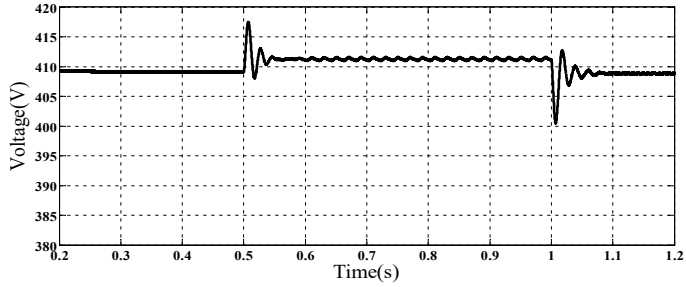

Fig. 10.The voltage variation with the virtual resistance in Case 1

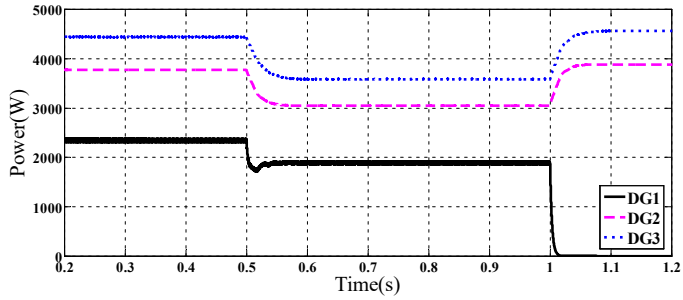

Fig. 11. The power sharing with the virtual resistance in Case 1

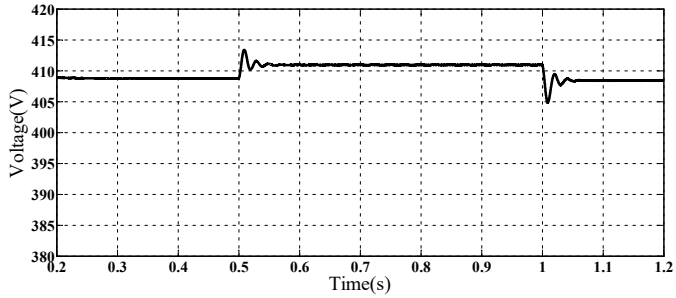

Fig. 12.The DC voltage with the nonlinear droop control method in Case 1

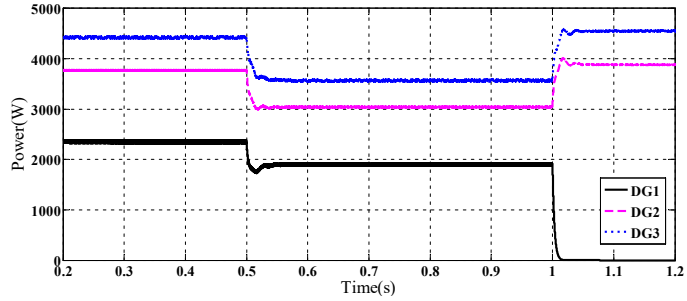

Fig. 13.The power sharing with the nonlinear droop control method in Case 1

This article has been accepted for publication in a future issue of this journal, but has not been fully edited. Content may change prior to final publication. Citation information: DOI 10.1109/TSG.2018.2797127, IEEE Transactions on Smart Grid

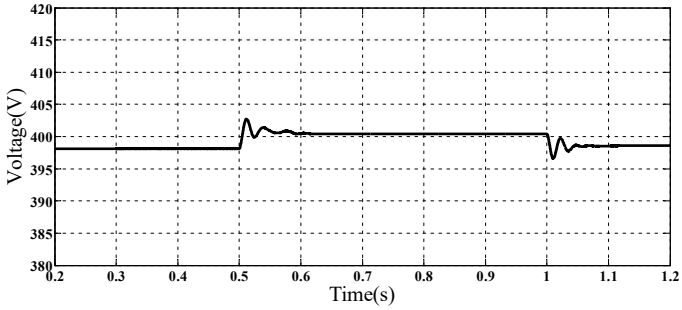

Fig. 14.The DC voltage with the proposed droop control method in Case 1

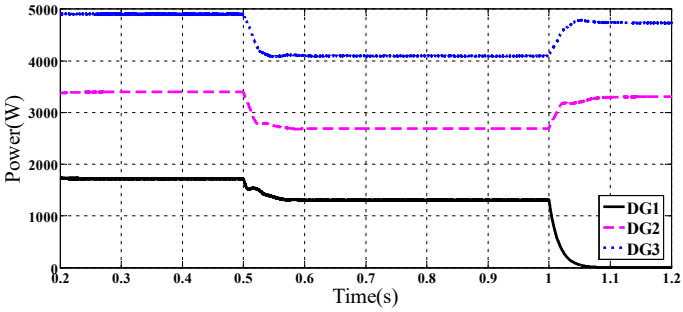

Fig. 15.The power sharing with the proposed droop control method in Case 1

Corresponding results obtained with the proposed droop controller are given in Fig. 14 - Fig. 15. Based on the simulation results from Fig. 8 - Fig. 15, the proposed method can realize better power sharing precision even under the load change and DG outage condition than the conventional droop strategy and the conventional droop controller with the nonlinear droop description or the virtual resistance compensation.

The DGs could share the loads nearly with the desired ratio of 1:2:3 using the proposed droop control no matter load decreases at 0.5s or DG1 drops off at 1.0s while the ratio of the powers shared with the traditional droop control is almost 1:1.6:1.9. Therefore, it is showed that the proposed droop scheme could share the loads effectively facing the cut down of loads and the outage of DGs.

However, the better power sharing could be obtained with a low bandwidth communication (LBC) network to exchange the information between converter units which have the same nominal ratings [13]. The output power becomes equality when the LBC control system is activated. But considering the communication delay, the stabilization time is longer than the proposed droop control method in this paper. And if with a high communication delay, the system becomes oscillatory and it is harder to keep the control system stable [13]. Aimed at an accurate result, the compensator for the virtual resistance is also considered and the fuzzy control is always the first key for this compensator [23, 25].

TABLE I
POWER SHARING WITH ALL THE DROOP CONTROL METHODS IN CASE 1

Line resistance 0.3Ω, 0.4Ω, 0.5Ω.		With the conventional droop		With virtual resistance		With the nonlinear droop		With the proposed droop	
		Output Power (W)	Proportional relation	Output Power (W)	Proportional relation	Output Power (W)	Proportional relation	Output Power (W)	Proportional relation
0s -0.5s	DG1	2367	1	2342	1	2350	1	1721	1
	DG2	3771	1.59	3779	1.61	3770	1.60	3406	1.98
	DG3	4408	1.86	4442	1.90	4420	1.88	4924	2.86
0.5s -1s	DG1	1907	1	1890	1	1900	1	1305	1
	DG2	3044	1.60	3049	1.61	3045	1.60	2689	2.06
	DG3	3558	1.86	3585	1.90	3565	1.88	4080	3.12
1s -1.5s	DG2	3891	2	3886	2	3880	2	3302	2
	DG3	4548	2.33	4568	2.35	4550	2.35	4732	2.87

The details of the power sharing with the three droop methods can be obtained from Table I. Moreover, a smaller voltage deviation can be obtained by the proposed droop control method than the other two droop control method. Although there is still voltage fluctuation in Fig. 14, but it can be shown that the deviation is smaller than the traditional droop control and permissible range ±5% of practical power system.

Case 2: Changes of Line Resistances

As well known, one practical issue of droop control is to deal with the impact from cable resistance and sensor discrepancy. In order to test the effective of the proposed droop controller, the sudden changes of line resistances in the DC MG are also considered.

At first, the line resistances are 0.3Ω , 0.4Ω and 0.5Ω respectively while the load is 8000W. At 0.5s, the resistances are changed to 0.2Ω , 0.4Ω , 0.6Ω and all remains 1Ω since 1.0s. Fig. 16, Fig. 17 and Fig. 18 illustrate the results of the power sharing with the conventional droop control, the droop control with the virtual resistance and the proposed droop control respectively. The details derived from the comparison are summarized in Table II.

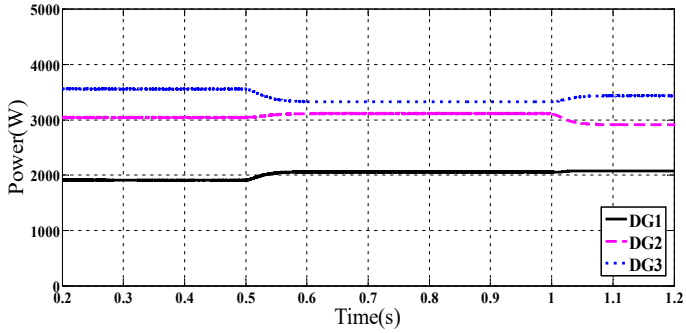

Fig. 16.The power sharing with the conventional droop control in Case 2

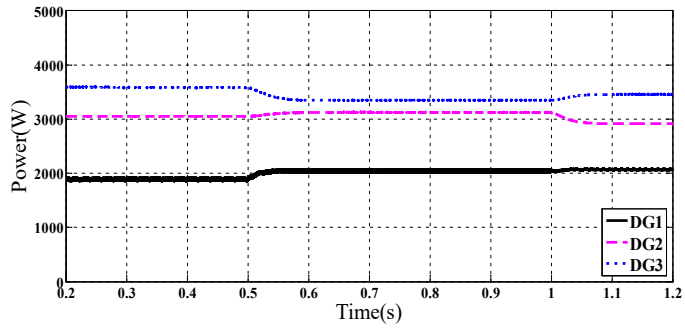

Fig. 17.The power sharing with the virtual resistance in Case 2

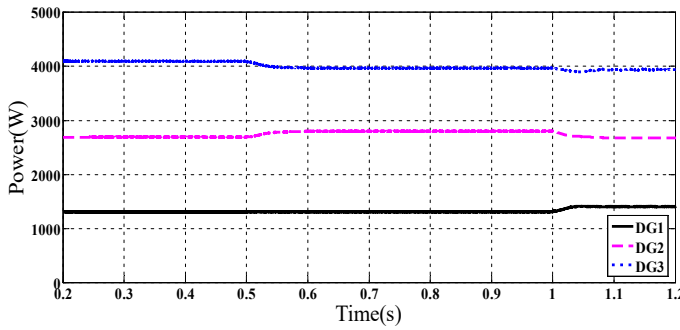

Fig. 18.The power sharing with the proposed droop control in Case 2

From Table II, both the conventional droop control and the proposed droop control cannot remove all the impact on the power sharing by the line resistance. But the proposed droop scheme brings more accurate power sharing than the other two droop control method. The ratio of the power sharing with the proposed droop method is more close to the ratio of DG nominal power, which is 1:2:3. When facing a wide range of the line resistance, the proposed sliding mode droop method can realize a better proportion even than the droop control with the virtual resistance under the same control parameters condition because of the robustness.

In order to further examine the capability of handling the parameters uncertainty in the microgrid, more possibilities of the

This article has been accepted for publication in a future issue of this journal, but has not been fully edited. Content may change prior to final publication. Citation information: DOI 10.1109/TSG.2018.2797127, IEEE Transactions on Smart Grid

line resistance are taken into account in this case. The transmission resistances are changed to 2.5Ω, 1.8Ω, 1.5Ω from 0.3Ω, 0.3Ω, 0.4Ω at 0.5s which is shown in Fig. 19. According to the result, the proposed T-S fuzzy sliding mode controller could compensate the uncertainties and disturbances well to derive accurate power sharing.

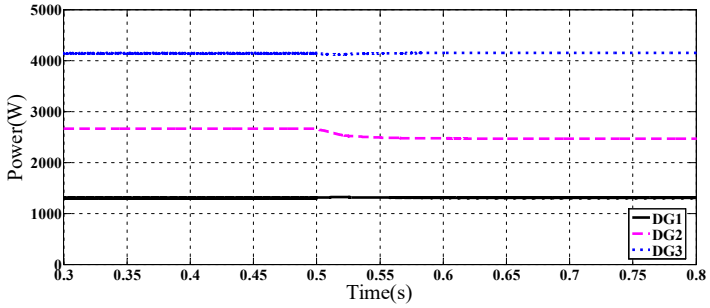

Fig. 19.The power sharing with the proposed droop control for variable resistances

TABLE II
POWER SHARING WITH ALL THE DROOP CONTROL METHODS IN CASE 2

Line resistance		With the conventional droop		With virtual resistance		With the proposed droop	
		Output Power (W)	Proportional relation	Output Power (W)	Proportional relation	Output Power (W)	Proportional relation
0s-0.5s	DG1	1910	1	1890	1	1305	1
	DG2	3043	1.59	3049	1.61	2689	2.06
	DG3	3558	1.86	3586	1.90	4080	3.12
0.5s-1s	DG1	2060	1	2045	1	1307	1
	DG2	3115	1.51	3125	1.53	2795	2.13
	DG3	3328	1.61	3346	1.64	3982	3.04
1s-1.5s	DG1	2078	1	2068	1	1369	1
	DG2	2913	1.40	2917	1.41	2676	1.95
	DG3	3438	1.65	3456	1.67	3940	2.88

V. CONCLUSION

The novel droop control strategy is proposed for accurate power sharing considering system parameters uncertainties and load disturbances. The technique is designed by using sliding mode controller based on T-S fuzzy model of the DC MG. The overall system stability can be assured. The conclusion is drawn that load changes of the DC MG can be regulated more adaptively. Meanwhile, the proportional load power sharing can be accurately achieved without any communication. The proposed method is verified in PSIM/Matlab simulation. Future extensions of the method can include nonlinear sliding mode droop control of multiple batteries or in AC/DC hybrid MG.

ACKNOWLEDGMENT

The authors would like to thank the National Natural Science Foundation of China (No.61403246), the National Key Research and Development of China (No. 2017YFB0903400), "Electrical Engineering" Shanghai class II Plateau Discipline and Shanghai Green Energy Grid Connected Technology Engineering Research Center (No.13DZ2251900).

APPENDIX

A. The Detail Parameters

The values used in the simulation are mentioned in the following Table.

TABLE III
VALUES FOR THE SIMULATION

Symbol	Description	Value
$\mathbf{K_{di}}$	droop coefficient of the proposed method	-0.6,-1.2,-1.8
$\mathbf{m_i}$	droop coefficient of conventional droop method	-0.004, -0.008, -0.012
$\mathbf{K_{vr}}$	The virtual resistance	-0.04
$\mathbf{K_{pv}}$	The ratio coefficient of the voltage controller	0.1
$\mathbf{K_{pi}}$	The ratio coefficient of the current controller	100
$\mathbf{K_{iv}}$	The integral coefficient of the voltage controller	0.01
$\mathbf{K_{Ii}}$	The integral coefficient of the current controller	0.25

The eigenvalues of $A_i - B_i K_i$ in DG1 are as,

Eig1=[-2214.2; -308.2; -136.3+215.6i; -136.3 - 215.6i; -59.9];
Eig2=[-2222.5; -308.8; -133.7 + 223.3i; -133.7 - 223.3i; -62.5];
Eig1=[-2231; -309.4;-131+231.8i;-131-231.8i; -65.1], and so on.

B. Takagi-Sugeno fuzzy model of the droop control process

The overall Takagi-Sugeno uncertain fuzzy model of the droop control system of the proposed DC microgrid is given by

$$\dot{x}(t) = \sum_{i=1}^{16} \{(A_i + \Delta A_i)x(t) + B_i u(t) + d(t)\} ,$$

where

$$A_1 = A_2 = \cdots = A_{16} , A_{i45} = [k_{Pi}(2I_{dgri} + 0.5V_{op}k_{Pv}) + 1]/C ,$$

$$A_{i54} = -\frac{k_{Pi}(1.5k_{Pv}V_{op} + I_{dgri}) + 1}{L} ,$$

$$A_i = \begin{bmatrix} -\omega_c & 0 & 0 & \omega_c I_{opi} & 0 \\ 1 & 0 & 0 & -1 & 0 \\ -1 & k_{Iv} & 0 & -k_{Pv} & -1 \\ -2 & -\frac{k_{Pi}k_{Iv}I_{dgri}}{C} & -\frac{k_{Ii}I_{dgri}}{C} & \frac{k_{Pi}k_{Pv}I_{dgri}}{C} & A_{i45} \\ 2 & \frac{k_{Pi}k_{Iv}V_{op}}{L} & \frac{k_{Ii}V_{op}}{L} & A_{i54} & -\frac{k_{Pi}V_{op} - r_l}{L} \end{bmatrix} ,$$

$$B = \begin{bmatrix} \omega_c V_{op} & 0 & 0 & -1/C & 0 \end{bmatrix}^T , B_1 = B_2 = \cdots = B_{16} ,$$

$$\Delta A_i = \begin{bmatrix} 0 & 0 & 0 & 0 & 0 \\ \Delta A_{i21} & 0 & 0 & 0 & 0 \\ \Delta A_{i31} & 0 & 0 & 0 & 0 \\ \Delta A_{i41} & \Delta A_{i42} & \Delta A_{i43} & \Delta A_{i44} & \Delta A_{i45} \\ \Delta A_{i51} & \Delta A_{i52} & \Delta A_{i53} & \Delta A_{i54} & \Delta A_{i55} \end{bmatrix}$$

$$\Delta A_{i21} = \frac{0.5}{k_{d1}\sqrt{\frac{\Delta P_i}{k_{d1}} + 0.25V_{op}^2}} - 1 , \Delta A_{i31} = \frac{0.5k_{pv}}{k_{d1}\sqrt{\frac{\Delta P_i}{k_{d1}} + 0.25V_{op}^2}} + 1 ,$$

$$\Delta A_{i41} = \frac{-0.5k_{pi}k_{pv}(I_{dgr} + \Delta I_{dgi})}{Ck_{d1}\sqrt{\frac{\Delta P_i}{k_{d1}} + 0.25V_{op}^2}} + 2 , \Delta A_{i42} = \frac{-k_{pi}k_{iv}\Delta I_{dgi}}{C} ,$$

$$\Delta A_{i43} = \frac{-k_{ii}\Delta I_{dgi}}{C} , \Delta A_{i44} = \frac{k_{pi}k_{pv}\Delta I_{dgi}}{C} ,$$

$$\Delta A_{i45} = \frac{-k_{pi}k_{pv}\sqrt{\frac{\Delta P_i}{k_{d1}} + 0.25V_{op}^2} + 2k_{Pi}\Delta I_{dgi} + k_{Pi}k_{Pv}\Delta V_{oi}}{C} ,$$

$$\Delta A_{i51} = \frac{0.5k_{pi}k_{pv}(V_{op} + \Delta V_{oi})}{Lk_{d1}\sqrt{\frac{\Delta P_i}{k_{d1}} + 0.25V_{op}^2}} - 2 , \Delta A_{i52} = \frac{k_{pi}k_{iv}\Delta V_{oi}}{L} ,$$

$$\Delta A_{i53} = \frac{k_{ii}\Delta V_{oi}}{L} , \Delta A_{i55} = \frac{-k_{pi}\Delta V_{oi}}{L} , d_i = [0 \;\; d_{i2} \;\; d_{i3} \;\; d_{i4} \;\; d_{i5}]^T ,$$

$$\Delta A_{i54} = \frac{k_{pi}k_{pv}\sqrt{\frac{\Delta P_i}{k_{d1}} + 0.25V_{op}^2} - k_{Pi}\Delta I_{dgi} - 2k_{Pi}k_{Pv}\Delta V_{oi}}{L} ,$$

where $i = 1, 2, \cdots 16$.

REFERENCES

[1]. R. Lasseter, "Microgrids" in Proc. IEEE Power Eng. Soc. Winter Meet.,2002, pp. 305−308.

[2]. S. K. Mazumder, M. Tahir and K. Acharya, "Master−slave current-sharing control of a parallel DC-DC converter system over an RF communication interface", IEEE Trans. Ind. Electron., vol. 55, no. 1, pp. 59-66, Jan. 2008.

[3]. M. N. Iyer, and M. C. Chandorkar, "A generalized computational method to determine stability of a multi-inverter microgrid,"IEEE Trans. Power. Electron., vol. 25, no. 9, pp. 2420-2432, Sept. 2010.

[4]. R. Majumder, B. Chaudhuri, A. Ghosh, and F. Zare, "Improvement of stability and load sharing in an autonomous microgrid using supplementary droop control loop," IEEE Trans. Power Syst., vol. 25, no. 2, pp. 796-808, May. 2010.

[5]. P. C. Loh, D. Li, Y. K. Chai and F. Blaabjerg, "Autonomous operation of hybrid microgrid with AC and DC subgrids″, IEEE Trans. Power Electron., vol. 28, no. 5, pp. 2214-2223, May. 2013.

[6]. P. H. Divshali and M. Abedi, "Decentralized cooperative control strategy of microsources for stabilizing autonomous VSC-based microgrids," IEEE Trans. Power Syst., vol. 27, no. 4, pp. 1949-1959, Nov. 2012.

[7]. J. C. Vasquez and J. M. Guerrero, "Adaptive droop control applied to voltage source inverters operating in grid-connected and islanded modes," IEEE Trans. Ind. Electron., vol. 56, no. 10, pp. 4088-4096, Oct. 2009.

[8]. Y. W. Li and C. N. Kao, "An accurate power control strategy for power-electronics-interfaced distributed generation units operating in a low-voltage multibus microgrid," IEEE Trans. Power Electron., vol. 24, no. 12, pp. 2977-2988, Dec. 2009.

[9]. F.Diaz, C.G.Moran, J. G.Aleixandre and A. Diez, "Scheduling of droop coefficients for frequency and voltage regulation in isolated microgrids," IEEE Trans. Power Syst., vol. 25, no. 1, pp. 489-496, Feb. 2010.

[10]. R. Billinton and R. Karki, "Capacity expansion of small isolated power systems using PV and wind energy," IEEE Trans. Power Syst., vol. 16, no. 4, pp. 892-7, Nov. 2001.

[11]. E. Barklund, N. Pogaku, M. Prodanovic, C. Hernandez-Aramburo, and T. C. Green, "Energy management in autonomous microgrid using stability constrained droop control of inverters," IEEE Trans. Power Electron., vol. 23, no. 5, pp. 2346−2352, Sep. 2008.

[12]. J. He and Y. W. Li, "An enhanced microgrid load demand sharing strategy," IEEE Trans. Power Electron., vol. 27, no. 9, pp. 3984–3995, Sep. 2012.

[13]. X. Lu, J. M. Guerrero, K. Sun and J. C. Vasquez, "An improved droop control method for DC microgrids based on low bandwidth communication With DC bus voltage restoration and enhanced current sharing accuracy," IEEE Trans. Power Electron., vol. 29, no. 4, pp.1800-1812, Apr. 2014.

[14]. D. De and V. Ramanarayanan, "Decentralized parallel operation of inverters sharing unbalanced and nonlinear loads," IEEE Trans. Power Electron., vol. 25, no. 12, pp. 3015−3025, Dec. 2010.

[15]. A. Engler and N. Soultanis, "Droop control in LV-grids," in Proc. IEEE Future Power Syst., Nov., 2005, pp. 1−6.

[16]. Y. Mohamed and E. Saadany, ″Adaptive decentralized droop controller to preserve power sharing stability of paralleled inverters in distributed generation microgrids," IEEE Trans. Power Electron., vol. 23, no. 6, pp. 2806−2816, Nov. 2008.

[17]. C. Wang, Y. Li, K. Peng, B. Hong and Z. Wu, "Coordinated optimal design of inverter controllers in a micro-grid with multiple distributed generation units," IEEE Trans. Power Syst., vol.28, no.3, pp.2679-2687, Aug. 2013.

[18]. X. Liu, P. Wang, and P. C. Loh, "A hybrid ac/dc microgrid and its coordination control," IEEE Trans. Smart Grid, vol. 2, no. 2, pp. 278-286, Jun. 2011.

[19]. J. M. Guerrero, J. C. Vasquez, J. Matas, L. G. de Vicuna, and M. Castilla, "Hierarchical control of droop-controlled ac and dc microgrids—a general approach toward standardization," IEEE Trans. Ind. Electron., vol. 58, no. 1, pp. 158-172, Jan. 2011

[20]. N. R. Chaudhuri and B. Chaudhuri, "Adaptive droop control for effective power sharing in multi-terminal DC grids," IEEE Trans. Power Syst., vol. 28, no. 1, pp. 21−29, Feb. 2013.

[21]. R. Eriksson, J. Beerten, M. Ghandhari, and R. Belmans, "Optimising dc voltage droop settings for ac/dc system interactions," IEEE Trans. Power Del., vol. 29, no. 1, pp. 362-368. Feb. 2014.

[22]. J. Beerten, R. Belmans, "Analysis of power sharing and voltage deviations in droop-controlled DC grids," IEEE Trans. Power Syst., vol. 28, no. 4, pp. 4588-4597, Feb. 2013.

[23]. H. Kakigano, Y. Miura and T. Ise, "Distribution voltage control for DC microgrids using fuzzy control and gain-scheduling technique," IEEE Trans. Power Electron., vol. 28, no. 5, pp. 2246-2258, May. 2013.

[24]. H. Bevrani and S. Shokoohi, "An intelligent droop control for simultaneous voltage and frequency regulation in islanded microgrids," IEEE Trans. Smart Grid., vol. 4, no. 3, pp. 1505-1513, Sept. 2013.

[25]. S. Eren, M. Pahlevanine, A.Bakhshai, "An adaptive droop DC-bus voltage controller for a grid-connected voltage source inverter with LCL filter," IEEE Trans. Power Electron., vol. 30, no. 2, pp. 547-559, Feb. 2015.

[26]. Q. Gao, L. Liu, G. Feng, Y. Wang and J. Qiu, "Universal fuzzy integral sliding-mode controllers based on T−S fuzzy models," IEEE Trans. Fuzzy Syst., vol. 22, no. 2, pp. 350-362. April 2014.

[27]. Q. Gao, X.-J. Zeng, G. Feng, Y. Wang, and J. Qiu, "T−S-fuzzy-model based approximation and controller design for general nonlinear systems," IEEE Trans. Syst.,Man, Cybern. B, Cybern., vol. 42, no. 4, pp. 1131−1142, Aug. 2012.

[28]. F. Zheng, Q.W.Wang, and T. Lee, "Output tracking control of MIMO fuzzy nonlinear systems using variable structure control approach," IEEE Trans. Fuzzy Syst., vol. 10, no. 6, pp. 686−697, Dec. 2002.

[29]. W. Cao and J. Xu, "Nonlinear integral-type sliding surface for both matched and unmatched uncertain systems," IEEE Trans. Autom. Control, vol. 49, no. 8, pp. 1355−1360, Aug. 2004.

[30]. M. Rubagotti, A. Estrada, F. Castanos, and L. Fridman, "Integral sliding mode control for nonlinear systems with matched and unmatched perturbations," IEEE Trans. Autom. Control, vol. 56, no. 11, pp. 2699−2704, Nov. 2011.

[31]. J. Zhang, P. Shi, and Y. Xia, "Robust adaptive sliding mode control for fuzzy systems with mismatched uncertainties," IEEE Trans. Fuzzy Syst., vol. 18, no. 4, pp. 700−711, Aug. 2010.

[32]. Y. W. Liang, S. D. Xu, D.C. Liaw, and C. C. Chen, "A study of T−S model-based SMC scheme with application to robot control," IEEE Trans. Ind. Electron., vol. 55, no. 11, pp. 3964−3971, Nov. 2008.

[33]. Tine L. Vandoorn, Bart Meersman, Jeroen D. M. De Kooning, and Lieven Vandevelde, ″Analogy Between Conventional Grid Control and Islanded Microgrid Control Based on a Global DC-Link Voltage Droop," IEEE Trans. Power Del., vol. 27, no. 3, pp. 1405-1414. Jul. 2012.

[34]. F. Chen, R. Burgos, D. Boroyevich, and W. Zhang, "A nonlinear droop method to improve voltage regulation and load sharing in DC systems," IEEE First International Conference on Dc Microgrids, pp. 45-50, 2015.

[35]. H. J. Avelar, W. A. Parreira, J. B. Vieira, L. C. G. de Freitas and E. A. A. Coelho, "A state equation model of a single-phase grid-connected inverter using a droop control scheme with extra phase shift control action," IEEE Trans. Ind. Electron., vol. 59, no. 3, pp. 1527−1537, Mar. 2012.

[36]. N. Pogaku, M. Prodanovic, and T. C. Green, "Modeling, analysis and testing of autonomous operation of an inverter-based microgrid," IEEE Trans. Power Electron., vol. 22, no. 2, pp. 613−625, Mar. 2007.

[37]. H.G. Zhang, F. S. Yang, "T-S model-based relaxed reliable stabilization of networked control systems with time-varying delays under variable sampling," International Journal of Fuzzy Systems, vol. 13, no. 4, pp. 260-269, Dec. 2011.

[38]. Q. P. Ha, Q. H. Nguyen, D. C. Rye and H. F. Durrant-Whyte, "Fuzzy sliding-mode controllers with applications," IEEE Trans. Ind. Electron., vol. 48, no. 1, pp. 38-46, Feb. 2001.